Population-Based Design of Mandibular Fixation Plates with Bone Quality and Morphology Considerations

Habib Bousleiman,[1] Tateyuki Iizuka,[2] Lutz-Peter Nolte,[1] and Mauricio Reyes[1]

[1]Institute for Surgical Technology and Biomechanics, University of Bern, Stauffacherstrasse 78, 3014 Bern, Switzerland; and
[2]Department of Cranio-Maxillofacial Surgery, University of Bern, Inselspital, 3010 Bern, Switzerland

Associate Editor Mona Kamal Marei oversaw the review of this article.

Abstract—In this paper we present a new population-based implant design methodology, which advances the state-of-the-art approaches by combining shape and bone quality information into the design strategy. The method may enhance the mechanical stability of the fixation and reduces the intra-operative in-plane bending which might impede the functionality of the locking mechanism. The computational method is presented for the case of mandibular locking fixation plates, where the mandibular angle and the bone quality at screw locations are taken into account. The method automatically derives the mandibular angle and the bone thickness and intensity values at the path of every screw from a set of computed tomography images. An optimization strategy is then used to optimize the two parameters of plate angle and screw position. The method was applied to two populations of different genders. Results for the new design are presented along with a comparison with a commercially available mandibular locking fixation plate (MODUS® TriLock® 2.0/2.3/2.5, Med-artis AG, Basel, Switzerland). The proposed designs resulted in a statistically significant improvement in the available bone thickness when compared to the standard plate. There is a higher probability that the proposed implants cover areas of thicker cortical bone without compromising the bone mineral density around the screws. The obtained results allowed us to conclude that an angle and screw separation of 129° and 9 mm for females and 121° and 10 mm for males are more suitable designs than the commercially available 120° and 9 mm.

Keywords—Orthopedic implant design, Population-based analysis, Computational anatomy, Mandibular locking fixation plate.

ABBREVIATIONS

CT	Computed tomography
d	Distance between adjacent screw holes
DVF	Deformation vector field
f	Objective functuion
H	Local voxel intensity
I	Intensity value
n	Number of sampled voxels along one screw path
N_r	Number of screws in one region
p	Number of image datasets
r	Specific anatomical region
R	Set of anatomical regions
T	Local bone thickness
α	Plate angle–mandibular or gonial angle
θ	Bone thickness
ω_θ, ω_I	Weighting factors

INTRODUCTION

The human mandible is a complex structure and a site of high incidence of traumatic or pathologic defects. Reconstruction of defects of the mandible using internal fixators is a common procedure in the general and specialized orthopedic wards. Similar to other sites, mandibular fixation plates are selected from a limited range of models provided by the manufacturers.[10] Therefore the need to intra-operatively adapt the implant to the patient-specific anatomy is almost always present, a delicate and time-consuming procedure that is prone to high inaccuracies.[3]

Manufacturing of internal fixators could range from the entirely patient-specific designs to the development of a universal set of implants from which the surgeon

Address correspondence to Habib Bousleiman, Institute for Surgical Technology and Biomechanics, University of Bern, Stauf-facherstrasse 78, 3014 Bern, Switzerland. Electronic mail: habib.bousleiman@istb.unibe.ch

selects the most suitable on a case-by-case basis. The former type is burdened with increased manufacturing and logistic costs, whereas the latter requires careful and sometimes excessive intra-operative adaptation to fit the implant to the anatomy of the patient being operated. A tradeoff lies in between the two extremes, the so-called population-based design. Current trends tend to pre-contour the implants to the average anatomy of the target population or to a template bone considered as representative of that population.[12,16,19] This approach, together with the development of locked internal fixators, reduced the need for plate bending.[5,12,18,19] However, in this design approach manufacturers tend to use small populations of cadaveric bones whose morphology does not necessarily reflect the actual differences in populations of patients.[16] Moreover, it has been shown to be suboptimal when fit criteria besides bone morphology and surface-to-surface distances are considered.[2,7]

Recent research presented population-based methods to improve the design of the shape of pre-contoured fixation plates.[2,7] In Kozic *et al.*,[7] an alteration of a commercially available proximal tibial implant was proposed based on optimization of surface distances using level-set segmentation in a statistical shape space. In Bou-Sleiman *et al.*,[2] an articulated model of the implant was used to minimize more clinically relevant metrics, namely the amount of bending and torquing required to adapt the implant to the anatomy of the patient undergoing the surgery (as opposed to minimizing surface distances). However, neither one of the approaches incorporates bone quality information into the design. Moreover, they both focus on the out-of-plane deformations and do not address the in-plane bending of the plates.

For the specific case of locking mandibular plates, in-plane bending is the most important type of deformation since it affects the shape of the screw holes and locking mechanism. Out-of-plane deformations are less important in this case because mandibular plates are relatively thin and hence easy to adapt to the patient anatomy. Therefore, for mandibular plates the angle between the mandibular body and ramus, referred to hereafter as mandibular or gonial angle, is of major importance.

In addition to the surface morphology, the mechanical properties of bone are a major criterion to be considered while designing implants,[15] especially in structures such as the mandible where the amount of bone is not in large supply. A well designed implant must present reduced risk of screw pullout and higher mechanical stability. Bone thickness and bone mineral density can be inferred from computed tomography (CT) images where bone porosity, bone density, and image intensity values are well correlated.[9,20] Moreover, it has been shown that the quality of cortical bone has a considerable positive

influence on the stability of the implant.[6] For the particular case of the mandibular reconstruction plate, the AO Foundation (Davos, Switzerland) recommends flushing the implant to the inferior edge of the body and posterior edge of the ramus. These regions are almost entirely composed of cortical bone.

In this paper we present a computational population-based design methodology of orthopedic fixators, which advances the state-of-the-art approaches by combining shape and bone quality information into the design strategy. The proposed methodology is presented for the specific case of mandibular locking plates. Of special interest are the in-plane pre-contouring and the bone thickness and intensity values at screw insertion sites. The implant parameters that we optimize are the plate angle and the distance between adjacent screw holes. In addition we present a comparison between the proposed design and a commercially available model. This paper is an extension of our previous preliminary work[1] where we presented the same method but with certain limitations. Our experimental dataset was limited in size and resolution and we did not consider differences in the anatomy between different genders.

In this study, we assume that there are potential morphological differences between males and females.[4,11,14] We also assume that the differences between gender groups would lead to different implant designs. Therefore, we separate the available population by gender and apply the design process on each group independently. We also use the obtained results to validate our assumption of gender differences. Furthermore, we apply the method on a larger number of high-resolution CT datasets.

METHODS

Experimental Data and Pre-Processing

A total of 80 CT images of the adult skull where the mandibles were manually segmented was used in this study. The CT images were acquired at different medical centers with varying machine settings. They were originally acquired for diagnostic purposes. Therefore, the approval of an ethics committee was not required. All patients signed an informed consent stating that the data might be used for future research. Anonymity of the datasets was observed. The age and gender distributions of the population are listed in Table 1. Each image is composed of $193 \times 351 \times 329$ voxels and a voxel spacing of 0.4 mm.

All images were initially rigidly aligned and resampled to the resolution specified above. Non-rigid registration was then applied in order to establish a voxel-wise correspondence between every image and a predefined reference. The populations were treated

TABLE 1. Distribution of subject age and measured mandibular angle within the gender-specific populations.

	Male	Female	
Count	41	39	
Age (years)			
Mean	61.7	68.1	
Median	65	71	
SD	14.6	15.3	Angle of standard plate 120.0
Angle (°)			
Mean	119.5	126.0	
Median	118.3	125.7	
SD	3.0	4.0	
Stat. sig. Male vs. Female	$p < 0.001$	***	

The angle of the standard commercially available plate is also listed.

similarly and independently. Therefore two reference images were selected, one from the male and one from the female populations. We used the non-rigid registration algorithm described in Seiler *et al.*[17] which was initially presented for mandibles and with a final aim toward implant design. The choice of the reference images is considered as integral part of the registration process and a pre-requisite to the method we present in this article. The algorithm applies local affine transformations onto subdivisions of the original anatomy. This is particularly beneficial for the registration of mandibles as it breaks down the complex morphology into simpler independent elements. The algorithm yields a deformation vector field (DVF) for every image relating voxels in the image to those in the reference *via* an anatomically meaningful correspondence.

Measurement of the Gonial Angle

A well-designed plate angle reduces the need of intra-operative in-plane bending and hence the risk of deforming the locking screw holes. In order to highlight possible differences among the gender-specific populations and to acquire an initial angle value for the angle optimization process, we measured the mandibular angle within the set of images in our database.

In order to digitally measure the mandibular angle, we manually placed a set of four landmark points on the reference mandible. Two landmarks were aligned with the left posterior edge of the ramus and the other two were aligned with the left inferior edge of the body of the mandible. We used the computed DVF to propagate the coordinates of the landmarks to all other images in the population. For every instance, the angle formed between the line connecting the two ramal landmarks and that connecting the landmarks

on the mandibular body was automatically calculated. Figure 1a illustrates this process graphically.

### Measurement of Bone Thickness and Intensity Values

Similarly, we placed a set of eight landmarks at the screw entry points on the reference image. This is analogous to the eight screw holes in the standard plate and consistent with the AO guidelines stating that at least three screws must be placed on either side of the fracture. We also placed a corresponding set of landmarks on the interior side of the mandible to delineate the paths of the screws.

For any particular combination of implant parameters (plate angle and distance between adjacent holes), the landmark configuration is modified accordingly and propagated to all instances of the population using the computed DVF. Geometrical constraints were integrated in the computation in order to ensure that the screw holes remain equidistant, that they are not misaligned, and that the plate angle is not affected by the varying mandibular angle due to DVF propagation. Additionally, a safety margin of 3 mm (consistent with the implant dimensions) was set around the screws in order to prevent any parts of the implant from being placed outside the bone.

The Euclidean distance between each pair of corresponding landmarks was computed. This represents the bone thickness at that particular screw insertion site. A 2 mm tube (diameter of a typical mandibular screws) was used to sample voxels between each pair of landmarks. The average intensity value computed along the sampled volume was used to represent the cortical bone quality at that location. Figure 2 shows a 3D view of the landmark configuration and the sampled volumes.

Anatomical Grouping

Based on recommendations of the AO Foundation and standards of anatomy, the plate and mandible were divided into three anatomically distinct regions, namely, the ramus, the angle, and the body of the mandible. The regions contain three, two, and three screw holes, respectively. Each region was treated separately and considered as a single unit during the optimization process and the analysis of the results. The two screws of the angle region were used to anchor the plate in place and remain fixed during the optimization. Therefore, changes in intensity values or bone thickness are not expected for that region. The configuration of the anatomical regions is illustrated in Fig. 1b.
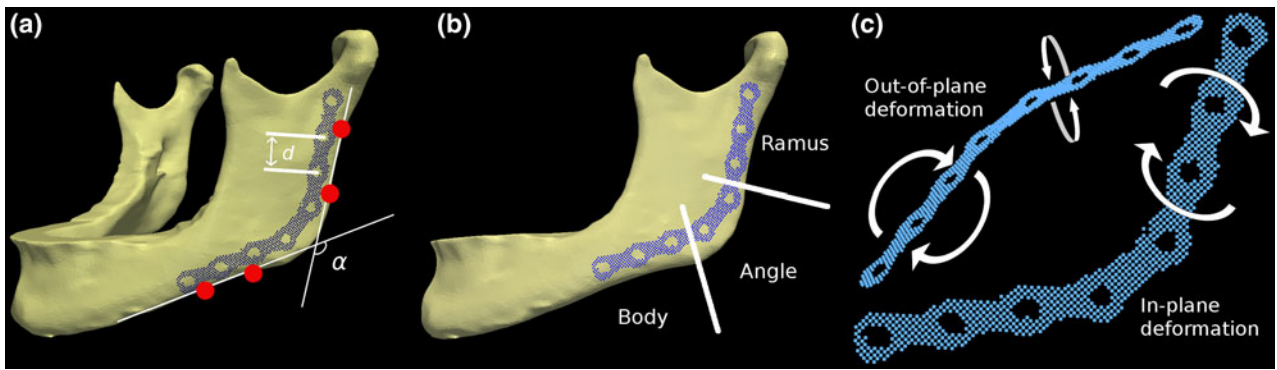
FIGURE 1. 3D view of the reference mandible with the standard fixation plate placed in its correct location. (a) Visible landmarks (red circles) used to measure the mandibular angle. (b) Anatomical grouping of the mandible and plate into three regions, namely, ramus, angle, and body of the mandible. (c) Illustration of the in-plane and out-of-plane deformations relative to the plate.
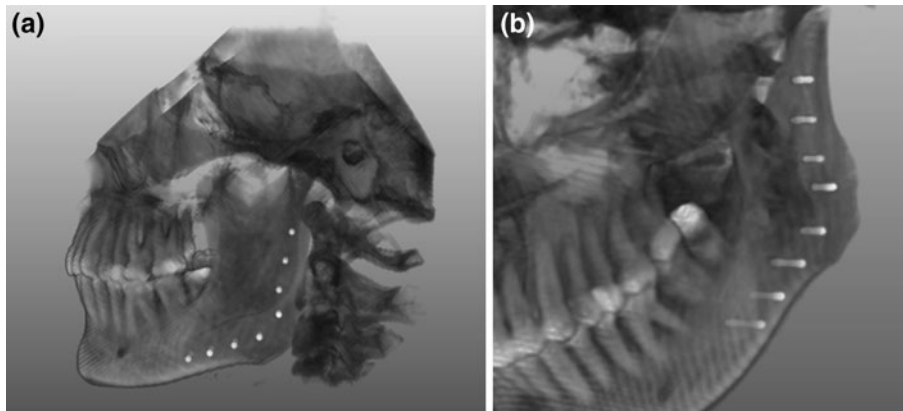
FIGURE 2. Volume rendering of the reference image showing the (a) landmarks corresponding to the screw sites of a 120° and 9 mm plate and (b) the paths of the screws along which the intensity values are sampled.

The Design Process

The mandibular plate was parameterized using two geometric features, in particular the plate angle α and the distance separating two adjacent screws d. The design criteria were the bone thickness and the intensity values per anatomical region $R = \{Ramus, Angle, Body\}$.

For every image in the database, the algorithm scans through the two-dimensional search space and for every pair of parameters computes the intermediate objective function

$$f(\alpha, d)_{im} = \omega_\theta \sum_{r \in R} \theta_r^{\alpha,d} + \omega_I \sum_{r \in R} I_r^{\alpha,d}. \qquad (1)$$

$f(\alpha,d)$ is composed of two components, namely, the thickness and the intensity components. Both terms are weighted according to their desired relative contribution. In Eq. (1), ω_θ and ω_I are the respective weighting factors. Both terms are normalized by their respective ranges of value per image to a unitless scale with values within [0, 1] in order allow for the two components of initially different units to be linearly combined.

The thickness component is the average of the bone thickness measured at all screw sites within one region and can be written as

$$\theta_{r \in R} = \frac{1}{N_r} \sum_{i=1}^{N_r} \tilde{T}_{r,i}, \qquad (2)$$

where N_r is the number of screws in one particular region and $\tilde{T}$ the normalized local bone thickness.

Similarly, the intensity component is the mean of the intensity values sampled along all screws within one region, or equivalently

$$I_{r \in R} = \frac{1}{N_r} \sum_{i=1}^{N_r} \left[\frac{1}{n} \sum_{j=1}^{n} \tilde{H}_j \right]_{r,i}, \qquad (3)$$

where n is the number of sampled voxels for every screw, and $\tilde{H}$ the normalized individual voxel intensity. The normalization step has an additional benefit, that is to circumvent the uncalibrated images and the different scanning and machine settings.

Calculating Eq. (1) for all images results in a vector of length equal to the total number of images p for

every combination of α and d. The final objective function to be maximized is but the magnitude of the obtained vectors. A traceable extensive search was used, thus eliminating the need for an optimization strategy such as gradient-based approaches. A formal representation of the total objective function is given as

$$f(\alpha, d)_{\text{total}} = \sqrt{\sum_{\text{im}=1}^{p} [f(\alpha, d)_{\text{im}}]^2}$$

$$= \sqrt{\sum_{\text{im}=1}^{p} \left[\omega_\theta \sum_{r \in R} \theta_r^{\alpha,d} + \omega_I \sum_{r \in R} I_r^{\alpha,d} \right]^2}. \quad (4)$$

APPLICATION, EVALUATION, AND RESULTS

The first step was to measure the mandibular angle in the population using the approach described above. The distributions of the measured gonial angles for each gender population are listed in Table 1. The angles of female mandibles are found to be larger than those of the males with a statistically significant difference. This result was obtained using both ANOVA and t test.[13] These findings were used to initialize and set the domain of the optimization along the angle parameter. We chose that value to be two standard deviations around the mean mandibular angle of the population with steps of one degree. This choice was based on the assumption that the measured data follow a Gaussian distribution, which was proven through the Lilliefors test of normality.[8] We constrained the distance between the screws by the screw hole geometry (6 mm) and an arbitrarily larger value (16 mm) with 1 mm steps. Since we did not have prior knowledge about the adequate weighting factors, we varied them to cover all possible combinations and repeated the computations for every pair (ω_θ, ω_I). The outcome of the optimization process was constant for $\omega_\theta \geq 0.5$ (i.e., $\omega_I \leq 0.5$) in the case of males, and $\omega_\theta \geq 0.2$ (i.e., $\omega_I \leq 0.8$) for females. These combinations are consistent with our design strategy to assign higher importance to the available thickness of the cortical bone. Varying the weighting factors allows for the designer to find the optimal combination for the specific implant and population under scrutiny. The computation time is in the range of few milliseconds per image. However, the main processing time is occupied by the loading and unloading of the images into memory.

We applied the optimization algorithm with the corresponding pair of optimal weighting factors on each population. Equation (4) reached its maximum value for $\alpha = 121°$ and $d = 10$ mm for males and $\alpha = 129°$ and $d = 9$ mm for females. The objective
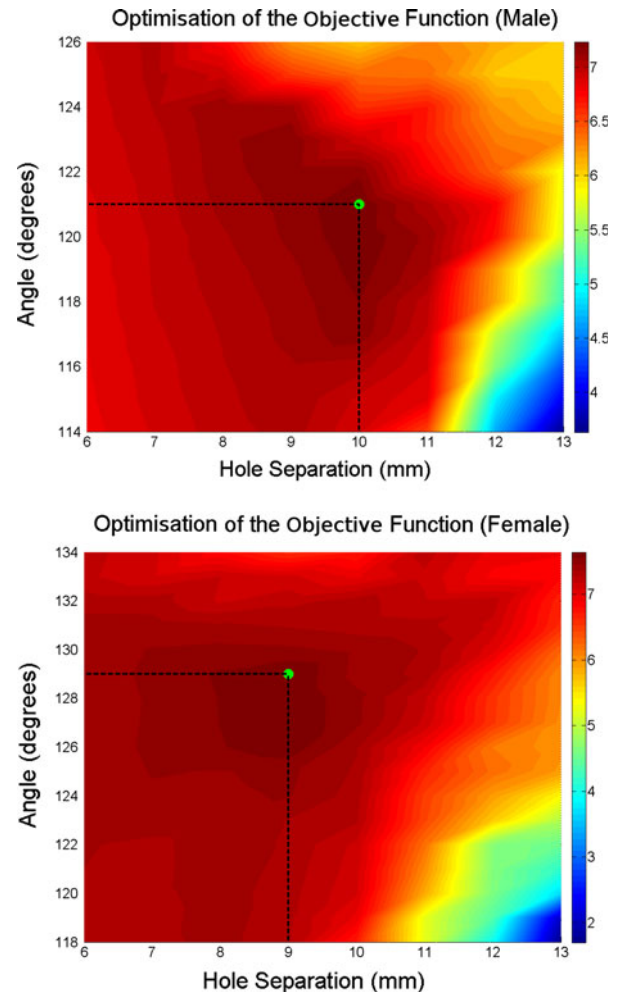
FIGURE 3. Surface plots of the objective function for the (*top*) male and (*bottom*) female populations against the 2-dimensional optimization space spanned by the design parameters α and d. The green circle is the peak value.

function is plotted in Fig. 3 against the 2D space of the design parameters.

In order to evaluate the new design, we generated implant configurations with the obtained parameters and compared it with that generated using the parameters of the commercially available design (low-profile MODUS® TriLock® 2.0/2.3/2.5, Medartis AG, Basel, Switzerland. $\alpha = 120°$ and $d = 9$ mm). We applied the same method in both cases and measured the resulting distribution of bone thickness along the screw insertion paths. We carried out two-tailed t-tests to calculate the statistical significance of the differences in the obtained results using a significance level of 0.05.[13] The results are listed in detail in Table 2. A graphical comparison of the geometries of the standard design and the designs proposed using the method presented herein is shown in Fig. 4.
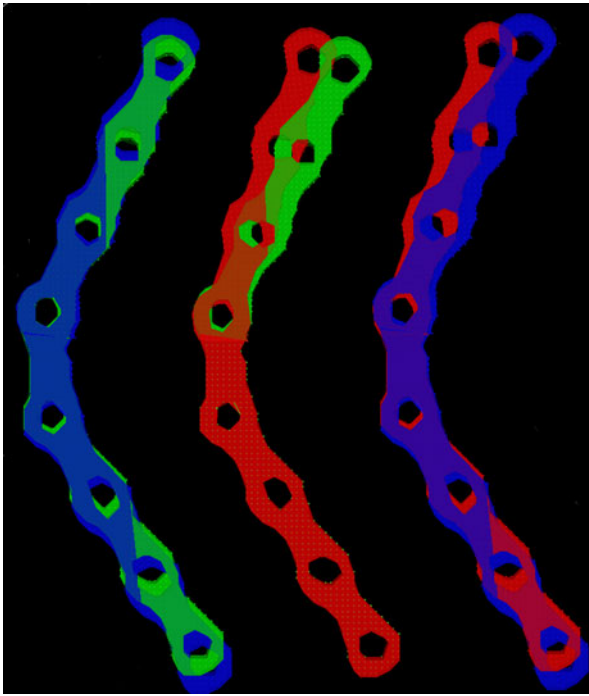
FIGURE 4. Overlay comparison of the geometries of the (*green*) standard and the proposed designs for (*blue*) males and (*red*) females.

DISCUSSION

In this paper we presented a new population-based orthopedic implant design methodology that combines shape and bone quality information into a single optimization process. The method was presented for the case of mandibular internal reconstruction plates. Of interest to the design were two parameters, namely the angle of the plate and the distance separating two consecutive screw holes. Using computational anatomy and image analysis techniques, the mandibular angle and the bone thickness and intensity values at screw paths were measured. This allowed us to formulate an optimization strategy to minimize the required intra-operative in-plane plate bending and maximize bone quality in and around the volumes that will be occupied by the screws. These two factors are to a large extent responsible for the success of the fixation.[3,6,15] We presented an evaluation of the proposed design by means of a comparison with a commercially available fixator. We used a larger database of CT images with higher resolution than that used in our previous study.[1] The image registration algorithm[17] that we used for pre-processing the data was specifically design for mandibles and associated implant design.

We postulated that there is a significant morphological difference between the two genders. To test this hypothesis, we divided our image database into two populations of opposite sexes. We measured the mandibular angle of every subject in each one of the populations of available CT images. We obtained a noticeable difference between the gonial angles of male and those of female subjects. This is consistent with the fact that males have sharper mandibular angle than females, a sexual dimorphism that has been reported by a number of studies.[4,11,14]

The difference between the measured gonial angle and that of the standard plate indicates that the latter is not optimal and has room for improvement. We used the methodology developed above to propose enhanced gender-specific plate designs. The proposed and the standard designs were compared in terms of available bone thickness and bone quality at screw locations. A statistically significant increase was measured for the new design in the bone thickness at screw insertion sites in the region of the mandibular body (males) and ramus (females). Statistically non-significant improvements were observed in the remaining regions for both bone thickness and intensity values at screw paths. In the cases of slight decrease in the sampled intensity values (male, ramus and body), the statistical significance of the changes was very low. As expected, and since the screws of the mandibular angle were fixed, no change was observed in that region.

The proposed designs proved through computational experiments that they are capable of performing better for a larger population span than the current commercial design. Within the population, there is a higher probability that the proposed implants cover areas of thicker cortical bone without compromising the bone mineral density around the screws. Though no clinical trials have been carried out yet, experiments using medical image analysis and computational anatomy methods allowed us to conclude that our design is methodologically sound and that statistically a plate with angle and screw separation of 129° and 9 mm for females and 121° and 10 mm for males are more suitable designs than the generic 120° and 9 mm.

The method presented herein can be extended to be applied on other implant types and for various anatomical sites. The length of the implant is not as important as its shape since in practice and according to the guidelines of the AO foundation, a plate longer than needed is intra-operatively cut to size. Therefore the length of the fixator was excluded from our analysis. The overall length of the plate will increase with increasing distance between the screw holes. Therefore, the respective effects will be correlated and redundant. We are aware that the length of the fixation and the location of the screws have a direct effect on the mechanical properties of the reconstruction and the force distribution over the locking mechanism.

TABLE 2. Comparison of the measured bone thickness and sampled intensity values at screw insertion sites for the standard and the proposed plate designs.

| | Standard | | Proposed | | | | |
	μ	σ	μ	σ	Impr. (%)	Stat. Sig.	p-value
Male							
Thickness (mm)							
Ramus	5.2	1.4	5.3	1.5	2	*n.s.*	0.08
Angle	5.7	1.8	5.7	1.2	0	*n.s.*	1
Body	9.2	2.3	9.6	2.1	4.3	***	<0.001
Intensity (HU)							
Ramus	579	228	571	226	−1.4	*n.s.*	0.19
Angle	722	193	722	193	0	*n.s.*	1
Body	696	289	694	286	−0.3	*n.s.*	0.59
Female							
Thickness (mm)							
Ramus	5.0	1.8	5.5	1.7	10	***	<0.001
Angle	6.3	1.4	6.3	1.4	0	*n.s.*	1
Body	10.7	2.1	10.7	2.1	0	*n.s.*	1
Intensity (HU)							
Ramus	589	234	592	215	0.5	*n.s.*	0.79
Angle	634	247	634	247	0	*n.s.*	1
Body	635	230	635	230	0	*n.s.*	1

The results are grouped by gender and by anatomical region (*n.s.*: not significant, μ: mean, σ: standard deviation).

However, we have set plans to closely examine this topic in a study involving mechanical and finite element analysis that are outside the scope of and complement this paper. We plan to compare the mechanical behavior of the standard and the proposed designs *in situ*, in terms of distribution of forces and stresses, and resistance to screw pullout. This could also be followed by clinical trials where the design method the mechanical simulations and tests can be validated in the operating theatre.

ACKNOWLEDGMENT

REFERENCES

[1]Bousleiman, H., C. Seiler, T. Iizuka, L.-P. Nolte, and M. Reyes. Population-based design of mandibular plates based on bone quality and morphology. In: Proceedings of 15th International Conference on Medical Image Computing and Computer-Assisted Intervention—MICCAI 2012, Part I, pp. 66–73.

[2]Bou-Sleiman, H., L. E. Ritacco, L.-P. Nolte, and M. Reyes. Minimization of intra-operative shaping of orthopaedic fixation plates: a population-based design. In: Proceedings of 14th International Conference on Medical Image Computing and Computer-Assisted Intervention—MICCAI 2011, Part II, pp. 409–416.

[3]Frankle, M. A., J. Cordey, M. D. Frankle, F. Baumgart, and S. Perren. A retrospective analysis of plate contouring in the tibia using the conventional 4.5 (narrow) dynamic compression plate. *J. Orthop. Trauma* 8:59–63, 1994.

[4]Franklin, D., P. O'Higgins, C. E. Oxnard, and I. Dadour. Sexual dimorphism and population variation in the adult mandible forensic applications of geometric morphometrics. *Forensic Sci. Med. Pathol.* 3:15–22, 2007.

[5]Goyal, K. S., A. S. Skalak, R. E. Marcus, H. A. Vallier, and D. R. Cooperman. Analysis of anatomic periarticular tibial plate fit on normal adults. *Clin. Orthop. Relat. Res.* 461:245–257, 2007.

[6]Hong, J., Y.-J. Lim, and S.-O. Park. Quantitative biomechanical analysis of the influence of the cortical bone and implant length on primary stability. *Clin. Oral Implants Res.* 23(10):1193–1197, 2011.

[7]Kozic, N., S. Weber, P. Büchler, C. Lutz, N. Reimers, M. Á. González, and M. Reyes. Optimisation of orthopaedic implant design using statistical shape space analysis based on level sets. *Med. Image Anal.* 14:265–275, 2010.

[8]Lilliefors, H. W. On the Kolmogorov–Smirnov Test for normality with mean and variance unknown. *J. Am. Stat. Assoc.* 62:399–402, 1967.

[9]Merheb, J., N. Van Assche, W. Coucke, R. Jacobs, I. Naert, and M. Quirynen. Relationship between cortical bone thickness or computerized tomography-derived bone density values and implant stability. *Clin. Oral Implants Res.* 21:612–617, 2010.

[10]Nagamune, K., Y. Kokubo, and H. Baba. Computer-assisted designing system for fixation plate. IEEE International Conference on Fuzzy Systems—FUZZ IEEE 2009, pp. 975–980.

[11]Oettlé, A. C., P. J. Becker, E. de Villiers, and M. Steyn. The influence of age, sex, population group, and dentition on

the mandibular angle as measured on a South African sample. *Am. J. Phys. Anthropol.* 139:505–511, 2009.

[12]Perren, S. M. Evolution and rationale of locked internal fixator technology. Introductory remarks. *Injury* 32(Suppl 2):B3–B9, 2001.

[13]Petrie, A. Statistics in orthopaedic papers. *J. Bone Joint Surg. Br.* 88:1121–1136, 2006.

[14]Ponyi, S., and G. Szabó. Statistical investigation of mandibular dimensions for the planning of a series of mandibular corpus replacements. *J. Craniofac. Surg.* 2:1049–2275, 1990.

[15]Schiuma, D., S. Brianza, and A. E. Tami. Development of a novel method for surgical implant design optimization through noninvasive assessment of local bone properties. *Med. Eng. Phys.* 33:256–262, 2011.

[16]Schmutz, B., M. E. Wullschleger, H. Noser, M. Barry, J. Meek, and M. A. Schutz. Fit optimisation of a distal medial tibia plate. *Comput. Methods Biomech. Biomed. Eng.* 14:359–364, 2011.

[17]Seiler, C., X. Pennec, and M. Reyes. Geometry-aware multiscale image registration via OBBTree-based polyaffine log-demons. In: Proceedings of 14th International Conference on Medical Image Computing and Computer-Assisted Intervention—MICCAI 2011, Part II, pp. 631–638.

[18]Taljanovic, M. S., M. D. Jones, J. T. Ruth, J. B. Benjamin, J. E. Sheppard, and T. B. Hunter. Fracture fixation. *Radiographics* 23:1569–1590, 2003.

[19]Wagner, M. General principles for the clinical use of the LCP. *Injury* 34(suppl. 2):B31–B42, 2003.

[20]Zhang, J., C.-H. Yan, C.-K. Chui, and S. H. Ong. Accurate measurement of bone mineral density using clinical CT imaging with single energy beam spectral intensity correction. *IEEE Trans. Med. Imaging* 29:1382–1389, 2010.